NASA TECHNICAL NOTE

NASA TN D-4692

NASA TN D-4692

MATHEMATICAL DETERMINATION OF GEOMETRICAL IMAGE ABERRATIONS IN SINGLE- AND DOUBLE-MIRROR SYSTEMS

by Martin G. Hurwitz and Hubert F. A. Tschunko

Electronics Research Center
Cambridge, Mass.

NATIONAL AERONAUTICS AND SPACE ADMINISTRATION • WASHINGTON, D. C. • OCTOBER 1968

MATHEMATICAL DETERMINATION OF GEOMETRICAL IMAGE ABERRATIONS IN SINGLE- AND DOUBLE-MIRROR SYSTEMS

By Martin G. Hurwitz and Hubert F. A. Tschunko

Electronics Research Center
Cambridge, Mass.

NATIONAL AERONAUTICS AND SPACE ADMINISTRATION

For sale by the Clearinghouse for Federal Scientific and Technical Information
Springfield, Virginia 22151 – CFSTI price $3.00

MATHEMATICAL DETERMINATION OF GEOMETRICAL IMAGE ABERRATIONS IN SINGLE- AND DOUBLE-MIRROR SYSTEMS

By Martin G. Hurwitz and Hubert F. A. Tschunko
Electronics Research Center

SUMMARY

The mathematical analyses to determine the image aberrations of single- and double-mirror systems are presented. The single mirrors, spherical and paraboloidal, are considered. Then, double-mirror systems with paraboloidal primary and hyperboloidal secondary are considered, along with higher aspherics of the secondary and tolerances in the relative positions of the mirrors. This investigation is a first step in the evaluation of the imaging performance of single- and double-mirror systems.

The general analysis available in the literature is not applicable without development for the special requirements of the present case. This special raytracing is the prerequisite needed later for the Fourier transformations which serve to derive the image performance data necessary to the determination of wave optical aberrations.

INTRODUCTION

Image aberrations of mirrors and mirror systems have been investigated by many authors. In general, the more recent investigations used the third and higher order theory of aberrations. In this treatment these theories are not used, and the different families of geometrical image aberrations are not considered.

The image aberrations of single- and double-mirror systems are analyzed. Three-dimensional analytical and numerical raytracing methods are used in the determination of the sizes and shapes of the images. Apertures are represented by points uniformly distributed on concentric aperture circles which are projected as a cluster of closed-image curves. The largest dimension of each cluster is taken to be the aberration value ε.

First, single imaging mirrors with both spherical and paraboloidal imaging surfaces are investigated. Special features of the image curves, including the catacaustic for the sphere, are considered. Then, double-mirror systems with paraboloidal primary and hyperboloidal secondary mirrors are treated. Finally, position tolerances in the distances between both mirrors are considered.

MATHEMATICAL ANALYSIS

Single Mirrors

Initially, single-mirror systems were considered using mathematical models of the spherical and paraboloidal mirrors. These models were developed to permit comparative investigations of aberrations of each mirror as a function of its focal number and angle of field.

Consider a three-dimensional Cartesian reference frame with the optical axis along the z axis. A single-mirror telescope is modeled by a portion of a sphere or paraboloid with its vertex at the origin, its axis coincident with the optical axis, and its center of curvature along the positive z axis (Figures 1 and 2). The equations of the surfaces are

$$\left.\begin{aligned} x^2 + y^2 + (1 - z)^2 - 1 &= 0 \\ x^2 + y^2 - 2z + z^2 &= 0 \end{aligned}\right\} \quad \text{(sphere)} \qquad (1)$$

and

$$x^2 + y^2 - 2z = 0 \qquad \text{(paraboloid)} \qquad (2)$$

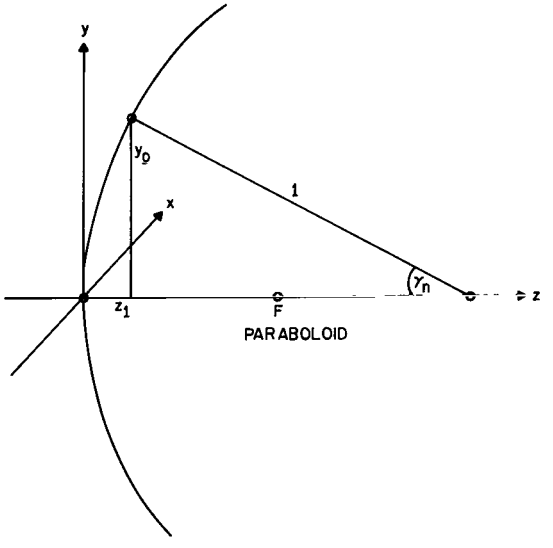

Figure 1

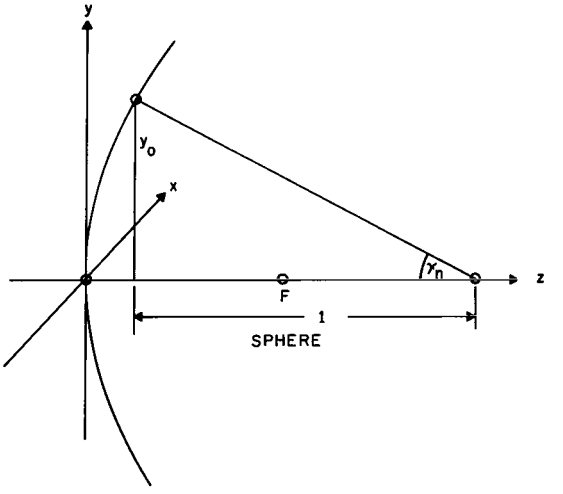

Figure 2

A point target at infinite distance emits light rays impinging on the aperture; these rays are reflected from the mirror

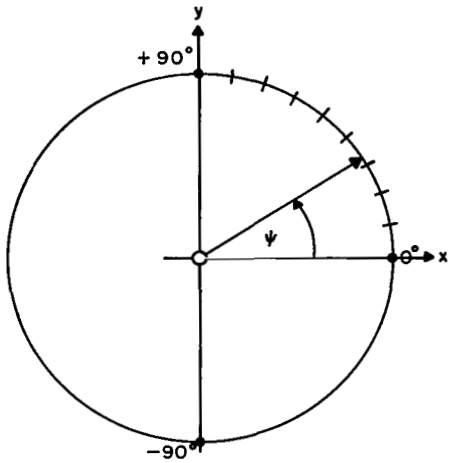

Figure 3

surface and imaged at a focal plane placed orthogonally to the optical axis at the focus of the paraboloid (0, 0, 0.5) where the focal length F_L is 0.5. The apertures, in either case, are represented by points uniformly distributed on concentric aperture circles representing different focal numbers (Figure 3).

In all the ray tracing calculations, directions are defined in terms of

$$\cos \alpha_j, \cos \beta_j, \text{ and } \cos \gamma_j.$$

These are the direction cosines related to the x, y, and z axes, respectively, and the subscripts j = i, n, or e are related to incident, normal, and exit rays, respectively. The exit ray directions may be determined when the incident rays and surface normals are known. Thus:

$$\left.\begin{aligned}
\cos \alpha_e &= \cos 2\alpha_n \cos \alpha_i + 2\cos \alpha_n (\cos \beta_n \cos \beta_i + \cos \gamma_n \cos \gamma_i) \\
\cos \beta_e &= \cos 2\beta_n \cos \beta_i + 2\cos \beta_n (\cos \gamma_n \cos \gamma_i + \cos \alpha_n \cos \alpha_i) \\
\cos \gamma_e &= \cos 2\gamma_n \cos \gamma_i + 2\cos \gamma_n (\cos \alpha_n \cos \alpha_i + \cos \beta_n \cos \beta_i)
\end{aligned}\right\} \quad (3)$$

Consider a ray approaching the mirror with angles γ_i, $\alpha_i = \pi/2$, $\beta_i = (\pi/2) - \gamma_i$.

The intersection of the mirror surface with its normal is determined from the focal number, i.e., focal length over aperture diameter equals F_N, as follows:

$$y_0 = \frac{0.5}{2F_N} \quad (4)$$

where y_0 is the radius of the aperture. The radius of curvature is assumed to be 1.0 and the focal length equal to 0.5. For the sphere:

$$y_0 = \sin \gamma_n \quad (5)$$

and for the paraboloid:

$$y_0 = -\tan \gamma_n. \tag{6}$$

The direction cosines of α_n, β_n are determined from

$$\cos \alpha_n = \sin \gamma_n \cos \psi \ , \quad \cos \beta_n = \sin \gamma_n \sin \psi \tag{7}$$

where ψ ranges as position angles over the aperture circle points. The direction cosines of the exit ray may now be determined from Eq. (3).

The exit ray is defined in terms of its intersection with the mirror (x_1, y_1, z_1), and its direction cosines as

$$\frac{x - x_1}{\cos \alpha_e} = \frac{y - y_1}{\cos \beta_e} = \frac{z - z_1}{\cos \gamma_e} \tag{8}$$

where

$$x_1 = y_0 \cos \psi \ , \quad y_1 = y_0 \sin \psi \tag{9}$$

while

$$z_1 = 1 - \cos \gamma_n \tag{10}$$

for the sphere and

$$z_1 = \frac{1}{2}\left(x_1^2 + y_1^2\right) \tag{11}$$

for the paraboloid.

This ray may be intersected with the focal plane $z = 0.5$ to define an image point. The entire image is obtained by allowing ψ to range over each aperture circle of constant radius. Different focal numbers provide different radii and different concentric aperture circles represent different focal numbers. All image curves together represent the image cluster, the whole geometrical image of the point object.

Special Image Points

The images from a paraboloidal single mirror display some interesting properties, such as a triple point and highest point, already pointed out by Crockett (ref. 1) and Plummer (ref. 2).

The triple points indicate a region in focal numbers and fields of view where the maximum sizes of the geometrical aberrations change from linear to quadratic dependence with field of view.

Each highest point indicates one limiting position within an image cluster. These points are necessary in determining the aberration sizes of the clusters, especially for larger focal numbers. Without these points no theoretical evaluation of the aberrations for higher focal numbers is possible.

These derivations are included because no exact determinations of these points may be found in the literature. A derivation of these points deals with relations between the angles of the incident ray and normal rays and is presented below.

Triple Point--The triple point is that point at which the image curve intersects itself for $\psi = 0^{\circ}$ and $\pm 90^{\circ}$.

Let $\psi = 0^{\circ}$. Then, from Eq. (7):

$$\cos \beta_n = 0, \quad \cos \alpha_n = \sin \gamma_n \tag{12}$$

and

$$\cos \gamma_i = 0, \quad \cos \beta_i = -\sin \gamma_i. \tag{13}$$

From Eq. (3):

$$\begin{aligned} \cos \alpha_e &= \sin 2\gamma_n \cos \gamma_i \\ \cos \beta_e &= \sin \gamma_i \\ \cos \gamma_e &= \cos 2\gamma_n \cos \gamma_i \end{aligned} \tag{14}$$

The intersection points (x_1, y_1, z_1) of the incident ray with the mirror surface are found to be

$$x_1 = -\tan \gamma_n , \quad y_1 = 0 , \quad z_1 = \frac{1}{2}\tan^2 \gamma_n \tag{15}$$

and the exit ray is then

$$\frac{x - x_1}{\cos \alpha_e} = \frac{y - y_1}{\cos \beta_e} = \frac{z - z_1}{\cos \gamma_e} \tag{16}$$

Thus, at $z = \frac{1}{2}$:

$$x = \frac{\cos \alpha_e}{\cos \gamma_e}\left(z - z_1\right) + x_1$$

$$= \tan 2\gamma_n\left(\frac{1}{2} - \frac{1}{2}\tan^2 \gamma_n\right) - \tan \gamma_n$$

$$= 0$$

and

$$y = \frac{\cos \beta_e}{\cos \gamma_e}\left(z - z_1\right) + y_1$$

$$= \frac{\tan \gamma_i}{2\cos^2 \gamma_n}\left(1 - \tan^2 \gamma_n\right)$$

$$= \frac{\tan \gamma_i}{2\cos^2 \gamma_n}$$

Now, let $\psi = -90^o$. Then:

$$\cos \beta_n = -\sin \gamma_n, \quad \cos \alpha_n = 0$$

$$\cos \alpha_i = 0, \quad \cos \beta_i = -\sin \gamma_i \tag{17}$$

From Eq. (3):

$$\cos \alpha_e = 0, \quad \cos \beta_e = \sin (\gamma_i - 2\gamma_n)$$

$$\cos \gamma_e = \cos (\gamma_i - 2\gamma_n). \tag{18}$$

The intersection of the incident ray with the surface now becomes

$$x_1 = 0$$
$$y_1 = -\tan \gamma_n \quad . \tag{19}$$

At $z = \frac{1}{2}$:

$$x = 0$$

$$y = \frac{\cos \beta_e}{\cos \gamma_e}\left(\frac{1}{2} - \frac{1}{2}\tan^2 \gamma_n\right) + \tan \gamma_n$$

$$= \frac{1}{2}\tan \left(\gamma_i - 2\gamma_n\right)\left(1 - \tan^2 \gamma_n\right) + \tan \gamma_n$$

$$= \frac{1}{2}\left[\frac{\tan \gamma_i - \tan 2\gamma_n}{1 + \tan \gamma_i \tan 2\gamma_n}\right]\left(1 - \tan^2 \gamma_n\right) + \tan \gamma_n \tag{20}$$

The two cases, $\psi = 0$ and $\psi = -90^\circ$, both yield $x = 0$. The two values of ψ result in the same image point, so the y values must be equated:

$$\frac{\tan \gamma_i}{2\cos^2 \gamma_n} = \frac{1}{2}\left[\frac{\tan \gamma_i - \tan 2\gamma_n}{1 + \tan \gamma_i \tan 2\gamma_n}\right]\left(1 - \tan^2 \gamma_n\right) + \tan \gamma_n \, . \tag{21}$$

This is simplified as follows:

$$\left(\tan \gamma_i\right)\left(\tan 2\gamma_n\right)\left(\tan \gamma_i - \tan \gamma_n\right) = 0 \tag{22}$$

Thus, the possible solutions:

$$\tan \gamma_i = 0, \quad \tan 2\gamma_n = 0, \quad \tan \gamma_i = \tan \gamma_n \tag{23}$$

yield the values

$$\left.\begin{aligned} \gamma_i &= \pm n\pi \qquad n = 0, 1, 2, \ldots \\ \gamma_n &= \pm\frac{n\pi}{2} \qquad n = 0, 1, 2, \ldots \end{aligned}\right\} \tag{24}$$

and

$$\frac{\tan \gamma_i}{\tan \gamma_n} = 1 \ . \tag{25}$$

Equation (25) provides the condition for the occurrence of the triple point.

Highest Point--The highest point of the image curve of a paraboloid mirror is found as follows.

Let the highest y coordinate of the image of a ray be denoted by y* and the corresponding point of intersection of the ray with the mirror by y_1. The highest point is then determined by minimizing y* - y.

From Figure 4:

$$\tan \gamma_e = \tan (2\gamma_n - \gamma_i)$$

$$= \frac{Ay^2 + 2y - A}{-y^2 + 2Ay + 1} \tag{26}$$

where

$$y = \tan \gamma_n$$

and (27)

$$A = \tan \gamma_i \ .$$

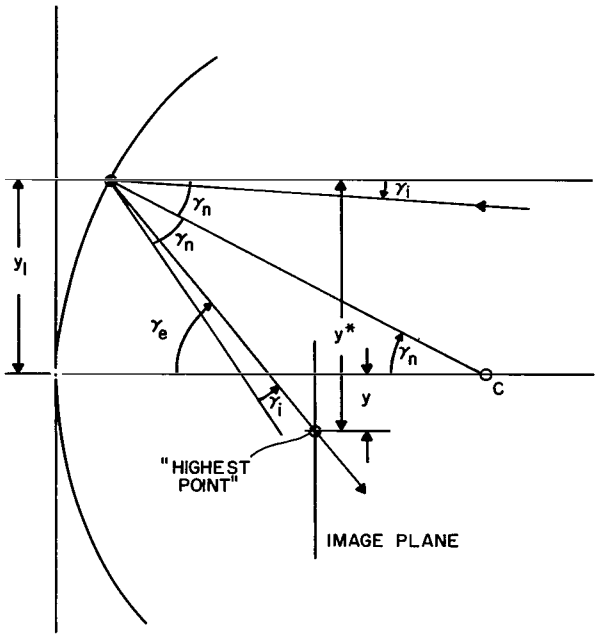

Figure 4

The value:

$$y^* - y = \tan \gamma_e (z_F - z_1) \ , \tag{28}$$

with z_F equal to the position of the focal plane, is to be minimized.

Taking

$$z_F = \frac{1}{2} \ , \qquad z_1 = \frac{y^2}{2}$$

and tan γ_e as above,

$$y^* - y = \frac{-\frac{Ay^4}{2} - y^3 + Ay^2 + y - \frac{A}{2}}{-y^2 + 2Ay + 1} - y \ . \tag{29}$$

For a minimum:

$$\frac{d}{dy}(y^* - y) = 0. \tag{30}$$

This results in the equation:

$$y^5 - 3Ay^4 - 2y^3 - 2Ay^2 - 3y + A = 0 \tag{31}$$

with

$$y \neq A \pm \sqrt{A^2 + 1}\ . \tag{32}$$

Then A can be found as

$$\tan \gamma_i = A = \frac{y^5 - 2y^3 - 3y}{3y^4 + 2y^2 - 1}\ . \tag{33}$$

When $y = \tan \gamma_n$ is small, $A \approx 3y$,

or

$$\tan \gamma_i \approx 3\tan \gamma_n \tag{34}$$

or

$$\frac{\tan \gamma_n}{\tan \gamma_i} \approx \frac{1}{3} \tag{35}$$

for small γ_n, and deviates from 1/3 as γ_n increases.

With this result, the highest point y* may be determined from the above. This equation (35) is the condition for the occurrence of the highest point.

Minimal Image Diameter of the Reflected Ray Bundle in the Catacaustic of a Spherical Mirror--In the case of the spherical single mirror, the incident rays form a blurred image created by the intersections of the tangents to the catacaustic curve with the optical axis, as shown in Figure 5.

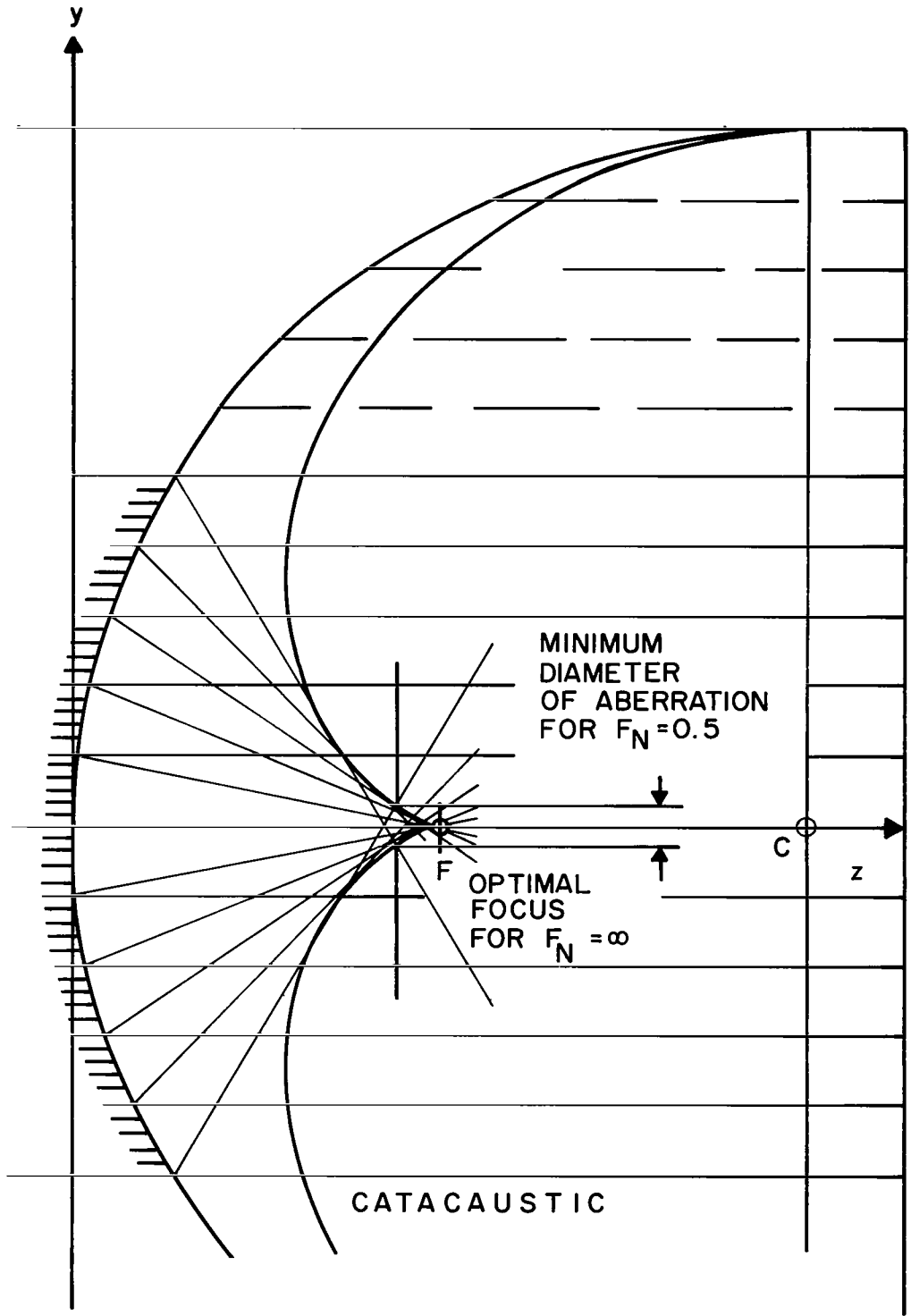
y
MINIMUM
DIAMETER
OF ABERRATION
FOR F_N = 0.5
C
z
F
OPTIMAL
FOCUS
FOR F_N = ∞
CATACAUSTIC

Figure 5

The catacaustic may be described parametrically as:

$$z = \frac{r}{4}(3\cos\alpha - \cos 3\alpha)$$
$$y = \frac{r}{4}(3\sin\alpha - \sin 3\alpha) \tag{36}$$

These equations may be combined to yield

$$\left[\left(\frac{4z}{r}\right)^2 + \left(\frac{4y}{r}\right)^2 - 4\right]^3 = 108\left(\frac{4y}{r}\right)^2 \tag{37}$$

where r is the radius of the sphere, and will be taken to be unity.

Further reduction of the above yields

$$y^2 = \left[\frac{4}{3}\left(z^2 + y^2 - \frac{1}{4}\right)\right]^3 \quad . \tag{38}$$

The reflected rays from a spherical mirror create a blurred image even when the incident rays are parallel to the optical axis. This occurs because the sphere does not image to a single focus as does the paraboloid, but each concentric zone of the spherical mirror has a different focal point for angles of incidence $\gamma_i = 0$. In this way, the catacaustic is formed as an envelope of the reflected rays. The rays from the largest aperture will be imaged in the focal plane, with the largest aberrations. The reflected ray is given by

$$y = -\tan\gamma_e(z - z_1) + y_1 \quad . \tag{39}$$

For the sphere:

$$\gamma_e = 2\gamma_n$$
$$y_1 = \sin\gamma_n \tag{40}$$
$$z_1 = -\cos\gamma_n \quad .$$

Substituting:

$$y = -\tan 2\gamma_n (z + \cos \gamma_n) + \sin \gamma_n \ . \tag{41}$$

Solving for z:

$$z = \frac{y - \sin \gamma_n}{-\tan 2\gamma_n} - \cos \gamma_n \ . \tag{42}$$

Substitution of this expression for z into the equation of the catacaustic then yields:

$$\sum_{i=0}^{6} A_i y^i = 0 \tag{43}$$

where

$$A_0 = \left(B^2 - \frac{1}{4}\right)^3$$

$$A_1 = \frac{6B}{T}\left(B^2 - \frac{1}{4}\right)^2$$

$$A_2 = \frac{3}{T^2}\left(5B^4 - \frac{3B^2}{2} + \frac{1}{16}\right) + 3\left(B^4 - \frac{B^2}{2} - \frac{5}{64}\right)$$

$$A_3 = \frac{B}{T^3}\left(20B^2 - 3\right) + \frac{12B}{T}\left(B^2 - \frac{1}{4}\right) \tag{44}$$

$$A_4 = \frac{3}{T^4}\left(5B^2 - \frac{1}{4}\right) + \frac{3}{T^2}\left(6B^2 - \frac{1}{2}\right) + 3\left(B^2 - \frac{1}{4}\right)$$

$$A_5 = \frac{6B}{T}\left(\frac{1}{T^2} + 1\right)^2$$

$$A_6 = \left(\frac{1}{T^2} + 1\right)^3$$

and

$$B = \frac{-\sin \gamma_n + \cos \gamma_n \tan 2\gamma_n}{\tan 2\gamma_n} \tag{45}$$

$$T = \tan 2\gamma_n \quad . \tag{46}$$

This equation in the variable y is solved by an iterative procedure, while noting that y and y_1 are opposite in sign. The diameter of the minimum bundle is taken as the aberration,

$$\varepsilon = 2|y| \tag{47}$$

To this minimal bundle diameter belongs a z-coordinate defining the optimal focal position for $\gamma_i = 0$. This focal position yields the focal length used to determine the image aberrations of the spherical mirror. For each focal number F_N a nominal value of the largest aperture diameter is used, thus yielding the optimal focal position length, or optimal focal length. For all smaller aperture circles of the same aperture, the same optimal focal length had to be used to assure the same focal plane in the same cluster of image curves.

The optimal focal plane positions OFP are presented as a function of focal number in the following table.

The OFP's are often obtained in a cumbersome and rather imprecise way. For this reason, they were computed with a higher number of figures to show the approach to the value of 0.5.

These values are necessary to compute the image aberrations of spherical mirrors over a larger range of focal numbers.

DOUBLE-MIRROR SYSTEM

First the ideal system is treated. This is a system of geometrically perfect paraboloidal primary and hyperboloidal secondary mirrors, without any higher surface aspherics, nor any provisions for tolerances in the mutual position between the two mirrors.

VALUES OF OPTIMAL FOCAL PLANE AS A FUNCTION OF FOCAL NUMBER FOR SPHERICAL MIRRORS

F_N	OFP	F_N	OFP
.5	0.43193 40028 65542	25.0	0.49998 12482 41999
.75	0.47669 87802 44569	32.0	0.49998 85552 53325
1.0	0.48754 48957 61076	50.0	0.49999 53123 90134
1.5	0.49465 18525 90037	64.0	0.49999 71389 36123
2.0	0.49702 66638 91014	80.0	0.49999 81689 28549
2.5	0.49810 72309 29950	100.0	0.49999 88281 18134
3.0	0.49868 93758 44114	150.0	0.49999 94791 65315
3.333	0.49879 90682 39857	200.0	0.49999 97070 30821
4.0	0.49926 48846 15958	250.0	0.49999 98124 99825
5.0	0.49953 01484 09819	256.0	0.49999 98211 86497
6.0	0.49967 39483 58068	320.0	0.49999 98855 59363
8.0	0.49981 67267 17227	400.0	0.49999 99267 57878
10.0	0.49988 27437 89342	500.0	0.49999 99531 34400
12.0	0.49991 85866 62538	512.0	0.49999 99552 96535
16.0	0.49995 42131 52687	1000.0	0.49999 99884 33952
20.0	0.49997 06988 32746	1024.0	0.49999 99889 19132

Ideal System

The double-mirror systems are Cassegrain systems. The primary is a paraboloid of revolution and the secondary is one sheet of a hyperboloid of two sheets. The paraboloid contains a central core in an area obstructed by the projection of the secondary mirror in the direction of γ_i, and of sufficient diameter to permit imaging of rays in a focal plane described

by $z = -B$, $B > 0$. Except for the core, the mirror will be the same as the single-mirror paraboloid described above.

In the ideal system, one focus of the hyperboloid coincides with that of the paraboloid, while the other focus is located at the point (0, 0, -B), the intersection of the focal plane with the optical axis (Figure 6).

The hyperboloid is described by the equation

$$z = h + \frac{C}{2}[(K + 1)(z - h)^2 + \rho^2] \tag{48}$$

where

$$\rho^2 = (x - x_0)^2 + (y - y_0)^2 , \tag{49}$$

x_0 and y_0 are displacements from the optical axis,

$$C = \frac{2\sqrt{-K}}{(K + 1)L} \tag{50}$$

is the vertex curvature of the hyperboloid,

$$K = -\left(\frac{M + 1}{M - 1}\right)^2 = -e^2 , \quad e > 1 , \tag{51}$$

where e is the eccentricity of the hyperboloid, and M is the imaging magnification of the secondary mirror,

$$L = 0.5 + B , \tag{52}$$

which is the distance from the secondary effective focal plane to the primary focus, and,

$$h = \frac{0.5 - MB}{M + 1} , \tag{53}$$

is a displacement along the optical axis.

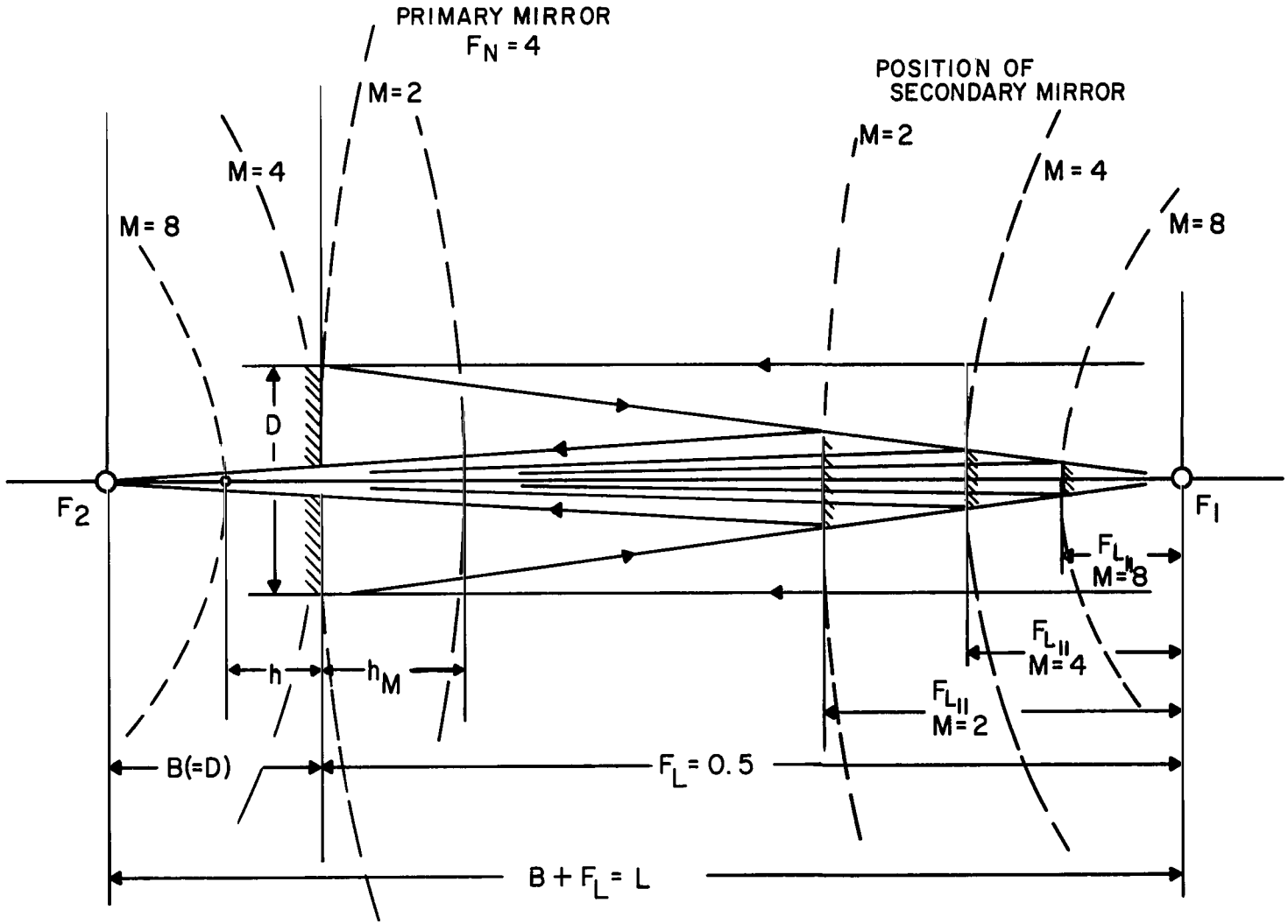
PRIMARY MIRROR
$F_N = 4$
POSITION OF
SECONDARY MIRROR
M=2
M=4
M=8
M=2
M=4
M=8
D
F_2
F_1
$F_{L_{II}}$
M=8
$F_{L_{II}}$
M=4
$F_{L_{II}}$
M=2
h
h_M
B(=D)
$F_L = 0.5$
$B + F_L = L$

Figure 6

The hyperboloid equation may be written as

$$\frac{(z - z_0)^2}{a^2} - \frac{\rho^2}{b^2} = 1 \tag{54}$$

where

$$a = \frac{1}{C(K + 1)} \tag{55}$$

$$b = a\sqrt{-(K + 1)} \tag{56}$$

are the semi-major and semi-minor axes, and

$$z_o = h + a \tag{57}$$

is the z coordinate of the center of the system. This provides a more common form for an elliptic hyperboloid of two sheets with center at (x_o, y_o, z_o).

A further simplification yields:

$$z = \pm \sqrt{a^2 - \frac{\rho^2}{K + 1}} + z_o \tag{58}$$

with the plus sign representing the right-hand sheet.

Double Mirror Geometry

The double-mirror system will create images in the back focal plane. The imaging process will be initially the same as that for the single mirrors up to reflection from the primary. The exit rays from the primary will intersect the secondary at points which must be determined. This determination is accomplished by simultaneous solution of the equation of exit ray with that of the hyperboloid using an iterative procedure. The intersection point will be called (x_2, y_2, z_2), and the value for z_2 should approximate the value B + h.

Once this point is established, the ray is reflected from this point, through the core of the paraboloid, and toward the

focal plane. The normal to the hyperboloid, H(x,y,z) = 0, at the intersection point is established for use in determination of the exit ray. This normal will have direction cosines

$$\left.\begin{aligned} \cos \alpha_n &= \frac{\partial H}{\partial x} t \\ \cos \beta_n &= \frac{\partial H}{\partial y} t \\ \cos \gamma_n &= \frac{\partial H}{\partial z} t \end{aligned}\right\} \tag{59}$$

with t determined as

$$t = \frac{1}{\sqrt{\left(\frac{\partial H}{\partial x}\right)^2 + \left(\frac{\partial H}{\partial y}\right)^2 + \left(\frac{\partial H}{\partial z}\right)^2}} \tag{60}$$

since

$$\cos^2 \alpha_n + \cos^2 \beta_n + \cos^2 \gamma_n = 1 \ . \tag{61}$$

The equation of the exit ray from the hyperboloid is then

$$\frac{x - x_2}{\cos \alpha_e} = \frac{y - y_2}{\cos \beta_e} = \frac{z - z_2}{\cos \gamma_e} \tag{62}$$

where $\cos \alpha_e$, $\cos \beta_e$, and $\cos \gamma_e$ are determined as in Eqs. (3), using the old exit angles as the new incidence angles, and the normals just established. The intersection point of this ray with the focal plane z = -B is then established, providing an image point (x_3, y_3, z_3).

The values y_3 may be reduced to a common origin so that comparison of values is facilitated. This is accomplished by subtracting a normalizing value from each y_3. Such normalizing values are computed as above with

$$\gamma_n = 0, \quad \gamma_i \neq 0, \quad \text{and} \quad F_N = F_N \text{ (nominal)}$$

and represents the intersection point of a ray through the center of the aperture with the secondary effective focal plane.

When this procedure has been done for all values of ψ for each aperture, the required images have been achieved as clusters of closed image curves. The largest dimention of each cluster is taken to be the aberration value ε.

Higher Aspherics

The hyperboloid will be described so as to include higher aspherics. These higher aspherics are introduced in such a way as to preserve radial symmetry of the surface about the optical axis. The inclusion of higher aspherics requires a modification of the equation of the surface,

$$z = z_0 + a\sqrt{1 - \frac{\rho^2}{a^2(K + 1)}} + \sum_{i=1}^{n} C_i \rho^{2(i + 1)} , \qquad (63)$$

with the C_i's as parameters to be determined. For this investigation, n is taken to be no more than 4 because the ranges of values to be considered render negligible the terms ρ^i with $i > 10$.

Tolerances

In addition to higher aspherics, the hyperboloid may be repositioned. A position change along the optical axis, an axial shift, will be denoted by δ, and the hyperboloid equation becomes

$$z = z_0 + \delta + a\sqrt{1 - \frac{\rho^2}{a^2(K + 1)}} + \sum_{i=1}^{n} C_i \rho^{2(i + 1)} \qquad (64)$$

and represents the secondary mirror, an aspheric hyperboloid displaced axially by an amount δ and laterally by amounts x_o and y_o, where x_o and y_o are now to be termed lateral shifts from the optical axis, as defined in Eq. (49).

The non-displaced case without higher aspherics is given by Eq. (64) with $\delta = x_o = y_o = 0$, and $C_i = 0$, $i = 1,\ldots,4$.

Finally, the hyperboloid may be tilted about its vertex. This tilting will be considered relative to the x and y axes, respectively, and jointly. Two-dimensional Cartesian coordinate systems, with x, y, and x', y' axes rotated through an angle θ relative to each other may be related as

$$x = x'\cos\theta + y'\sin\theta$$

$$y = -x'\sin\theta + y'\cos\theta \quad . \tag{65}$$

To achieve rotation of the system, the on-axis hyperboloid is shifted along the optical axis a distance,

$$\Delta = h + \frac{2}{C(K + 1)} + \delta \tag{66}$$

so that its origin coincides with that of the coordinate system. The hyperboloid is rotated first about y with angle θ, then about x with angle ϕ, and finally shifted back to its original vertex position. The equation of the hyperboloid with tilting is

$$[(z - \Delta)\cos\phi + (x - x_o)\sin\phi]\cos\theta + (y - y_o)\sin\theta$$

$$= a\left[\sqrt{1 + \frac{(\rho')^2}{b^2}} - 1\right] + f(\rho') \tag{67}$$

where

$$f(\rho') = \sum_{i=1}^{n} C_i(\rho')^{2(i + 1)} \tag{68}$$

and

$$(\rho')^2 = [(\Delta - z)\sin\phi + (x - x_o)\cos\phi]^2$$
$$+ \{-[(z - \Delta)\cos\phi + (x - x_o)\sin\phi]\sin\theta$$
$$+ (y - y_o)\cos\theta\}^2 \qquad (69)$$

Equation (67) will be rewritten as

$$H(x,y,z) = 0 \qquad (70)$$

where

$$H(x,y,z) = [(z - \Delta)\cos\phi + (x - x_o)\sin\phi]\cos\theta$$
$$+ (y - y_o)\sin\theta - a\left[\sqrt{1 + \frac{(\rho')^2}{b^2}} - 1\right]$$
$$- f(\rho') \qquad (71)$$

Optimum Axial Focus with Axial Shift Tolerance

In an ideal, double-mirror system, a parallel bundle of light approaching the primary mirror with $\gamma_i = 0$ would create a point image on the optical axis in the focal plane. (When $\gamma_i \neq 0$, aberrations are formed in the focal plane image.) If, in addition, tolerances in axial shift are introduced, it becomes necessary to find the optimal position for the focal plane, as the image with minimal aberrations no longer occurs at Z = -B, the secondary focus of the original hyperboloid.

The optimal focal plane position was evaluated as follows. For $\psi = 90^o$, the corresponding ray was traced as above, and imaged in each of two focal planes separated by a distance Z_B. This was done as a function of the focal number F_N; the ray

corresponding to the minimum value of F_N was intersected with the rays corresponding to $F_N + n\Delta(F_N)$, with $\Delta(F_N)$ an increment, for n = 1,2,... until an intersection was obtained which provided the minimum aberration value.

An iteration was then performed to ensure the realization of the actual minimum aberration. The position on the optical axis corresponding to these minimum aberrations was taken to be the focal plane position.

COMPUTATIONS

The given analyses provide the necessary geometrical skeleton for the numerical evaluation of image aberrations for the implementation on digital computers.

The computations were done using FORTRAN IV on the IBM-7049 II of NASA-ERC.

REFERENCES

1. Crockett, C.W.: The Parabolic Mirror, Astrophys. J., vol. 7, p. 362, 1898.
2. Plummer, H.C.: On the Images Formed by a Parabolic Mirror, Monthly Notices RAS, p. 352, 1902.

National Aeronautics and Space Administration
Electronics Research Center
Cambridge, Massachusetts, May 1968
125-22-02-33

NATIONAL AERONAUTICS AND SPACE ADMINISTRATION
WASHINGTON, D. C. 20546

OFFICIAL BUSINESS

FIRST CLASS MAIL

POSTAGE AND FEES PAID
NATIONAL AERONAUTICS AND
SPACE ADMINISTRATION

POSTMASTER: If Undeliverable (Section 158 Postal Manual) Do Not Return

"The aeronautical and space activities of the United States shall be conducted so as to contribute . . . to the expansion of human knowledge of phenomena in the atmosphere and space. The Administration shall provide for the widest practicable and appropriate dissemination of information concerning its activities and the results thereof."

— NATIONAL AERONAUTICS AND SPACE ACT OF 1958

NASA SCIENTIFIC AND TECHNICAL PUBLICATIONS

TECHNICAL REPORTS: Scientific and technical information considered important, complete, and a lasting contribution to existing knowledge.

TECHNICAL NOTES: Information less broad in scope but nevertheless of importance as a contribution to existing knowledge.

TECHNICAL MEMORANDUMS: Information receiving limited distribution because of preliminary data, security classification, or other reasons.

CONTRACTOR REPORTS: Scientific and technical information generated under a NASA contract or grant and considered an important contribution to existing knowledge.

TECHNICAL TRANSLATIONS: Information published in a foreign language considered to merit NASA distribution in English.

SPECIAL PUBLICATIONS: Information derived from or of value to NASA activities. Publications include conference proceedings, monographs, data compilations, handbooks, sourcebooks, and special bibliographies.

TECHNOLOGY UTILIZATION PUBLICATIONS: Information on technology used by NASA that may be of particular interest in commercial and other non-aerospace applications. Publications include Tech Briefs, Technology Utilization Reports and Notes, and Technology Surveys.

Details on the availability of these publications may be obtained from:

SCIENTIFIC AND TECHNICAL INFORMATION DIVISION

NATIONAL AERONAUTICS AND SPACE ADMINISTRATION

Washington, D.C. 20546